Characteristics of Soy Protein Isolate-Montmorillonite Composite Films

Jung-Eun Lee,[1] Ki Myong Kim[2]

[1]*Division of Food Bioscience & Technology, College of Life Sciences and Biotechnology, Korea University, Seoul, Korea*
[2]*R&D Team, Jeonnam Biofood Technology Center, Naju, Korea*

Received 1 October 2008; accepted 25 March 2009
DOI 10.1002/app.31316
Published online 22 June 2010 in Wiley InterScience (www.interscience.wiley.com).

ABSTRACT: Soy protein isolate/montmorillonite (SPI/MMT) nanocomposite films were prepared in which MMT was used as a nanofiller at 0, 3, 6, 9, 12, and 15 wt % relative to SPI dry weight. Effects of MMT on film properties including tensile strength, elongation at break, total soluble matter, water vapor permeability, and oxygen permeability were assessed. X-ray diffraction patterns were determined, and morphologies of SPI and the SPI-MMT composite films were visualized by scanning electron microscopy. Mechanical and barrier properties were improved by evidenced increases in tensile strength and modulus, and decreases in permeability to water vapor and oxygen. MMT concentrations of 3%–12% were optimal for improving functional properties of the composite films. X-ray diffraction and scanning electron microscopy examinations revealed the formation of an intercalated and exfoliated structure on the addition of MMT into the SPI matrix. We conclude that intercalated and exfoliated MMT silicates enhance mechanical and barrier properties of SPI films. © 2010 Wiley Periodicals, Inc. J Appl Polym Sci 118: 2257–2263, 2010

Key words: biopolymers; nanocomposites; mechanical properties; barrier; nanolayers

INTRODUCTION

The preparation of blends or conventional composites using inorganic or natural fillers are among the techniques used to improve some of the properties of biodegradable polymers. Thermal stability, gas barrier properties, strength, low melt viscosity, and slow biodegradation rate are among the properties that can be improved by these multiphase systems. Reinforcement of biodegradable polymers in nanometric dimensions produces nanocomposites, which has attracted research interest due to their potential value in the design of eco-friendly applications. Systems with structural features on the nanoscale level have substantially different physical, chemical, and biological properties from their macroscopic counterparts. Their use is changing the understanding of biological and physical phenomena in food packaging and other systems. For example, the addition of 5% (by weight) nano-sized clays significantly increases the mechanical and thermal properties of nylons.[1] The most widely studied type of polymer-clay nanocomposites is a class of hybrid materials composed of organic polymer matrices and organophilic clay fillers. Despite a great deal of research, improvement of the properties of such biopolymer-based films has been marginal.

Most biodegradable polymers have excellent properties comparable to many petroleum-based plastics and are readily biodegradable, which make them an attractive potential alternative to commodity plastics. This potential as a bio-plastic is presently tempered by their high water solubility, high hydrophilicity, brittleness, low heat distortion temperature, high gas permeability, and low melt viscosity, which restricts their general use. Modification of the biodegradable polymers through innovative technology is desirable, but presents a formidable challenge for materials scientists.

Biodegradable and edible food packaging films made of soy protein, starch, and chitosan have been studied and developed. Among these biopolymers, soy protein films are effective barriers to the passage of lipid, oxygen, and carbon dioxide (CO_2). However, the inherent hydrophilicity of proteins and the substantial amount of plasticizer added in the film creation process are drawbacks, because protein films perform poorly as moisture barriers and mechanical packaging material. Several studies have concentrated on improving mechanical and barrier properties of soy protein films utilizing chemical or natural additives,[2,3] physical treatments,[4–6] and enzymatic treatments.[7–9] Improvement in mechanical and barrier properties of biopolymer films has been limited, which has hampered their use in the food industry.

Correspondence to: K. M. Kim (kimhusker@korea.ac.kr).
Contract grant sponsor: Korea Research Foundation Grant funded by Korea Government (MOEHRD); contract grant number: KRF-2007-259-F00016.

Nanoreinforcement of pristine polymers to prepare nanocomposites has already proven to be an effective way to improve these properties concurrently. Tunc et al.[10] prepared gluten/montmorillonite (MMT) nanocomposite films by the casting method. The presence of MMT led to a significant reduction of the water sensitivity of wheat gluten-based films toward water vapor and aroma compounds. Whey protein isolate (WPI)-based composite films with three different types of nano-clays were prepared using a solution casting method, and their physical and antimicrobial properties were determined to better understand the effect of nano-clay type on film properties.[11] Rhim et al.[12] also prepared soy protein isolate (SPI)-clay mineral composite films and investigated the film properties. SPI has been well studied as a replacement for petroleum-based film materials because of its high film-forming ability but has not been investigated concerning changes of mechanical properties according to MMT concentration in films. To this end, the present study was undertaken to improve the barrier and mechanical properties of SPI film by incorporating the organophilic clay (MMT) into SPI films to form a composite solution. Beneficial alterations in mechanical properties including tensile strength (TS) and elongation at break (E), and barrier properties including water vapor permeability (WVP), oxygen permeability (OP), and total soluble matter (TSM) were observed.

MATERIALS AND METHOD

Film preparation

Five grams of SPI powder (Supro 620; Protein Technologies International, St. Louis, MO) was dispersed in 100-mL distilled water with 2.5 g (50% w/w of SPI) of glycerin (Sigma-Aldrich, St. Louis, MO). The powder was fully dissolved into solution by magnetically stirring at room temperature. The solution was heated at 75°C for 15 min and adjusted to a pH of 10.00 ± 0.01 using 0.1 *N* sodium hydroxide (Shinyo Pure Chemicals, Tokyo, Japan) to slightly denature the protein.[6] Sodium (Na)-MMT (0, 3, 6, 9, 12, and 15% w/w of SPI) was dissolved in the SPI solution at room temperature by vigorous magnetic stirring. The resulting SPI/MMT solution was homogenized at 11,000 rpm for 5 min, sonicated at 25°C for 15 min to exfoliate MMT layers, and filtered through Cheesecloth Wipes™ (VWRR Scientific Products, Chicago IL) to remove any bubbles. The final SPI/MMT solution was poured on a 25 cm × 25 cm Teflon-coated glass plate and dried at room temperature for 24 h. The dried film was peeled off and was conditioned at 25°C and 50% relative humidity for 48 h.

TS and E determinations

TS and E were both measured using a Model 5565 universal testing machine (Instron, Canton, MA) following the guidelines of ASTM Standard Method D 882-91.[13] The size of each specimen was 2.54 cm × 10 cm. Thickness of each film was determined to an accuracy of ±1 μm by measurement at five randomly selected locations using a Model ID-C112 digital micrometer (Mitutoyo, Kawasaki, Japan). The initial grip separation was set at 50 mm, load cell of 500 N, and cross-head speed of 100 mm/min. TS was calculated (mega Pascal; MPa) by dividing the maximum load (*N*) by the initial cross-sectional area (m^2) of the specimen. *E* was calculated as the ratio of the final length of the point of sample rupture to the initial length of a specimen (50 mm) as a percentage. TS and *E* tests for each type of film were replicated five times.

TSM determination

TSM was expressed as the percentage of film dry matter dissolved during immersion in distilled water for 24 h. Film pieces (20 × 20 mm) were placed in 50 mL beakers containing 30 mL of distilled water. Each beaker was covered with Parafilm™ 'M" wrap (American National Can, Chicago, IL) and stored at 25°C for 24 h. Dissolved dry matter was determined by discarding the water from the beakers and drying the remaining film in an air-circulating oven at 105°C for 24 h. The weight of the dissolved dry matter was calculated by subtracting the weight of insoluble solid matter from the initial weight of solid matter.[2] TSM tests for each type of film were replicated three times.

Water vapor permeability determination

Five film samples were tested for each type of film. WVP ($g \cdot m/m^2 \cdot h \cdot Pa$) was calculated as:

$$WVP = (WVTR \cdot L)/\Delta p$$

where WVTR is the measured water vapor transmission rate ($g/m^2 \cdot h$) through a film sample, *L* is the mean film sample thickness (m), and Δp is the partial water vapor pressure difference (Pa) between the two sides of the film sample. WVTR was determined gravimetrically using a modification of ASTM Method E 96-95.[14] Each film sample was mounted on a polymethylmethacrylate cup filled with 16 mL of distilled water up to 1.03 cm from the film's underside. Cups were placed in an environmental chamber set at 25°C and a relative humidity of 50%. A fan operating in the chamber moved the air over the surface of the films to remove the permeating

water vapor. The weights of each cup were recorded six times at 1-h intervals. Linear regression was used to estimate the slope of this line in g/h. WVP was calculated by a corrective equation.

OP determination

OP of SPI/MMT nanocomposite films was measured using a MOCON OX-TRAN® Model 2/60 (MOCON, Minneapolis, MN). Before testing, all specimens were conditioned at 25°C and 50% relative humidity for 48 h, and their thickness was determined using an ID-C112 digital micrometer (Mitutoyo). Samples were masked on the cell using creases. The test area and thickness of each film was 10 cm^2 and 0.09 ± 0.01 mm, respectively. The carrier gas was 98% N_2 and 2% hydrogen, and the test gas was pure O_2. The flow of the carrier and test gases was 10 mL/day and 20 mL/day, respectively. Testing was performed at 23°C under 0% relative humidity according to ASTM D 3985. OP determinations for each type of film were replicated three times.

Wide-angle x-ray scattering

Wide-angle XRD was used to determine basal d-spacing and recorded using small-angle x-ray scattering (SAXS) with a General Area Detector Diffraction System (GADD; Bruker AXS, Karlsruhe, Germany) with Cu Kα radiation (λ = 1.5406 Å) generated 45 mA and an operating voltage of 40 kV. Diffraction spectra were obtained over a 2θ range 0–40° in steps of 0.02° and an exposure time of 300 s.

Scanning electron microscopy (SEM)

Film surface and cross section morphology was examined using SEM. Selected films were individually mounted onto aluminum stubs with double-sided tape and sputtered coated to a thickness of 200 Å using a Desk II Sputter (Denton Vacuum, Moorestown, NJ). Selected hand-fractured samples were individually mounted on stubs with double-sided adhesive tape after freezing by immersion in liquid nitrogen. Images were taken using a JSM-5410LV scanning electron microscope (JEOL, Tokyo, Japan), using an accelerating voltage of 15 kV and 350x magnification.

Statistical analyses

ANOVA tables were generated for TS, *E*, WVP, TSM, and OP as a function of level of added MMT using the General Linear Model (GLM) program package of the Statistical Analysis System (SAS Institute, Cary, NC). Significantly ($P < 0.05$) different treatment means were separated using the Duncan's multiple range test.

RESULTS AND DISCUSSION

TS and *E* determinations

TS and *E* determinations of SPI/MMT composite films are summarized in Figure 1. TS and *E* values of SPI films devoid of MMT were 2.87 ± 0.27 MPa and 168.5 ± 15.0%, respectively. The TS of SPI/MMT composite films increased significantly ($P < 0.05$) as MMT concentration increased up to 15% (w/w SPI). The highest TS value (8.73 ± 0.76 MPa) was obtained by adding 15% (w/w SPI) of MMT into the film forming solution, which was approximately three times higher than control SPI film (0% MMT). At a high level of clay, ultrasonically treated samples appeared to give significant improvement of mechanical properties compared to convenient dispersing in starch solution.[15] Elongation of SPI-MMT composite films decreased dramatically from 168.5% ± 15.4% to 26.8% ± 4.0%. The lowest value was observed at 15% MMT, although the value was not significant compared to the value obtained at 9% MMT ($P > 0.05$). Further addition of Na-MMT over 15% resulted in the aggregation of MMT particles in SPI solution. Similar phenomenon was also found. Tunc et al.[10] experienced difficulty of mixing and spreading the film forming solution because of high viscosity. TS and *E* of polymer films including biopolymers are changed when clay is an included component. In one study, the mean TS values of SPI films composed of 10% Na-MMT increased significantly ($P < 0.05$) by 25%[12] and TS values of wheat gluten-MMT composite film increased by 2.5 times

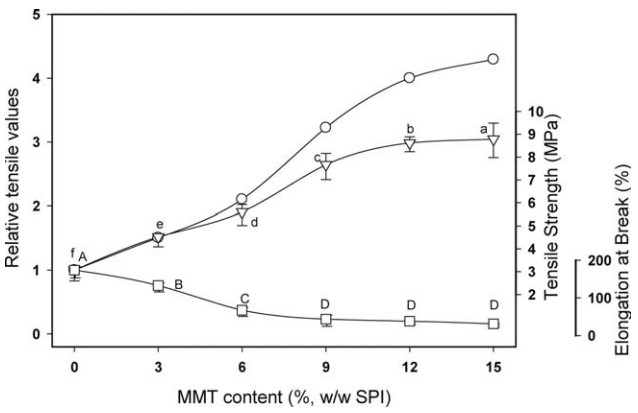

Figure 1 Mechanical properties of SPI/MMT nanocomposite films containing various concentrations of MMT. Young modulus (○), relative tensile strength (▽) and relative elongation at break point (□). a-f, A-D, Any two values followed by the same letter are not significantly ($P < 0.05$) different by Duncan's multiple range test.

when 5% MMT was incorporated.[10] Increased TS and decreased *E* of polylactide (PLA) nanocomposites incorporating MMT have been reported.[16] Starch/MMT nanocomposites can also enhance mechanical properties with increasing clay concentration up to 5%,[17] as are the mechanical properties of chitosan films with increasing clay concentration (<5%).[18] In this study, the mechanical properties of SPI/MMT nanocomposite films were also similarly enhanced at increasing clay concentrations. Mechanical properties including modulus and yield stress increase with increasing filler content.[19] In the latter study, the Young's Modulus was 4.1 times and the yield stress was 1.8 times greater for MMT composite films as compared with films devoid of MMT. In another study, polyacrylonitrile (PAN)/Na-MMT (Na-MMT)/SiO_2 nanocomposites were synthesized and the change of storage modulus according to MMT loading ratio in film was observed; storage modulus increased with increasing nano-material loading to a maximum value, which was followed by a decrease.[20] Improvement in tensile modulus by the incorporation of rigid fillers in wheat gluten polymer has been observed.[10] Collectively, the previous and present observations support the view that in polymers containing nano-materials, the nano-material does more than merely occupying spaces in the polymer network. Rather, interactions between the polymeric matrix and layered silicates via the formation of hydrogen bonds improve the overall mechanical strength of the polymer film.

TSM

TSM was not significantly different ($P > 0.05$) between samples (Table I). TSM of biopolymer films is generally evaluated for its integrity level, which is an essential determination when a cross-linking agent is added to increase the integrity of a film. Presently, MMT did not participate as a cross-linking agent, but as a filler when added to SPI films. The absence of significance between the samples and control indicates that SPI-MMT composite films have a similar integrity to the control, consistent with a stable localization of the MMT layers in SPI polymers. SPI films that incorporate clay display improved water resistance as evidenced by a decreased water solubility value.[13] A decrease in water solubility of 56% was evident when organic clay was added 10% to SPI films. Measurements of the water sensitivity of wheat gluten have demonstrated that water uptake into films increase as more clay is incorporated,[14] consistent with the hydrophilic character of MMT.

TABLE I
Total Soluble Matter of SPI-MMT Composite Film According to MMT Content

MMT Content (%, w/w of SPI)	Total Soluble Matter (%, w/w of Dry Film)
0	28.6 ± 2.54[a]
3	29.9 ± 0.87[a]
6	28.2 ± 0.79[a]
9	29.4 ± 0.46[a]
12	29.0 ± 0.29[a]
15	29.8 ± 0.81[a]

[a] Any two values followed by the same letter are not significantly ($P < 0.05$) different by Duncan's multiple range test.

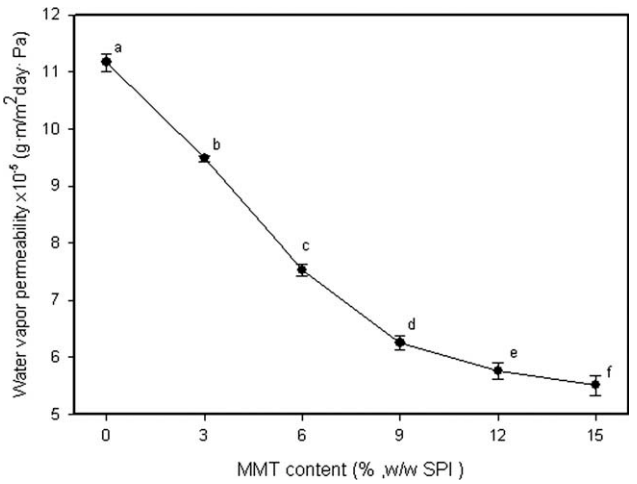

Figure 2 WVP of SPI/MMT composite films according to MMT content. a-f, Any two values followed by the same letter are not significantly ($P < 0.05$) different by Duncan's multiple range test.

WVP

WVP decreased significantly ($P < 0.05$) as MMT content increased in SPI films (Fig. 2). The WVP of SPI devoid of MMT was 11.2 ± 0.14 (x10^{-5} g·m/m^2·day·Pa), whereas WVP of SPI-MMT films containing 15% MMT decreased to 5.5 ± 0.17 (x10^{-5} g·m/m^2·day·Pa). This implies that MMT is well spaced in SPI polymers and effectively blocks the passage of water vapor. Biopolymers have a low capacity as a packaging film barrier because of their irregular polymeric network structure. Biopolymer films that contain MMT are of interest to food scientists as packaging films because of the reported improvement of barrier properties in biopolymer/MMT composite films. WVP of wheat gluten/MMT films were reported to decrease significantly after incorporation of MMT.[10] Permeability is controlled by diffusion and sorption; the reduction of the water vapor permeability can be attributed to a change in solubility rather than to a change in diffusivity

because of the lower availability of the hydrophilic site for water vapor by establishment of hydrophilic interactions between proteins and nanoclays.[14] According to TSM results in the present study, nanoclays may interact with SPI proteins, because the addition of a considerable amount of nanoclays did not affect TSM as compared to control SPI films. These results imply that hydrophilic sites available to bind water vapor in SPI films are lower than in control films, which results in decreased WVP. Contrary to this view, WVP values obtained with polymer-layered silicate nanocomposite models indicates that the clay platelets can effectively act as geometrical obstacles in the polymer matrix.[21,22] Further studies will be necessary to clarify the nature of film permeability.

OP determination

The effect of nanoclays on barrier properties of SPI films was investigated for O_2. The addition of MMT to SPI affected the OP of the SPI films over the range of studied MMT concentrations (Fig. 3). Comparison of the OP between SPI films in the absence and presence of Na-MMT demonstrated that the presence of Na-MMT enhanced OP. Interestingly, high OP was observed with SPI films at 15% MMT content (Fig. 3). Nanocomposite SPI films containing 3% MMT exhibited considerably reduced permeability, whereas films containing 15% MMT exhibited increased OP. This could be attributed to the superior level of organoclay intercalation achieved at Na-MMT levels of 3%–12% compared with 15% MMT. An investigation of O_2, N_2, and CO_2 permeability of low density polyethylene and a sodium ionomer of poly (ethylene-co-methacrylic acid) films after addition of MMT reported decreased gas permeability as the organoclay content increased in both polymers,[23] which agrees with our results. Generally, for polymers that are chemically identical, gas permeability increases as polymer crystallinity decreases.[24] However, the effect of the polar groups of SPI and the ionic clay clusters more than compensate for the decreased barrier resistance brought by the lower crystallinity of the SPI polymer. SPI is composed by amino acids containing ionic functional groups, which adopt various ionic states according to solvent types. Exfoliated clay can stably incorporate in the network of SPI polymers by interacting with ionic functional groups of SPI molecule with increasing concentration, until saturating conditions are achieved.

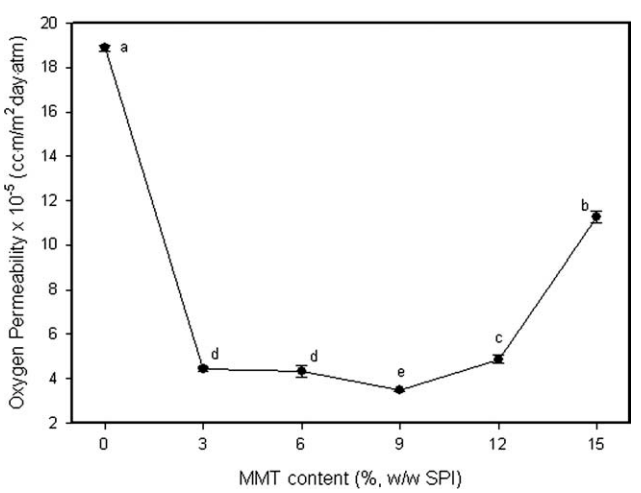

Figure 3 OP of SPI/MMT composite films according to MMT content. a-e, Any two values followed by the same letter are not significantly ($P < 0.05$) different by Duncan's multiple range test.

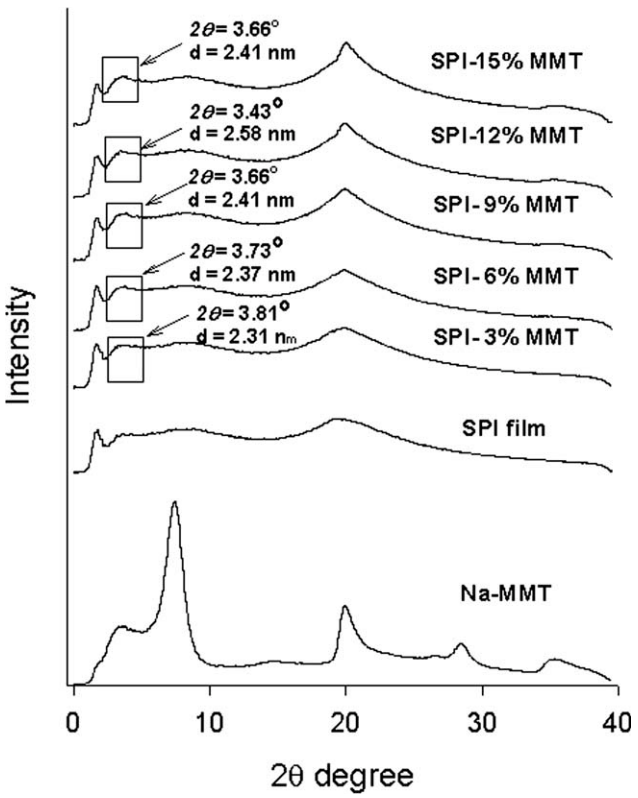

Figure 4 Effects of MMT content on XRD patterns of SPI films.

XRD

XRD elucidates the spacing between ordered layers of clay via the presence of the d_{001} or basal spacing.[25] Pure Na-MMT normally exhibits a peak associated with a spacing of $2\theta \approx 8^\circ$ and $2\theta \approx 20^\circ$[22]. The absence of this basal peak is commonly regarded as evidence for a high dispersion of clay platelets, whereas a peak associated with a higher spacing indicates an intercalated nanocomposite. Incorporation of MMT to SPI film was associated with the

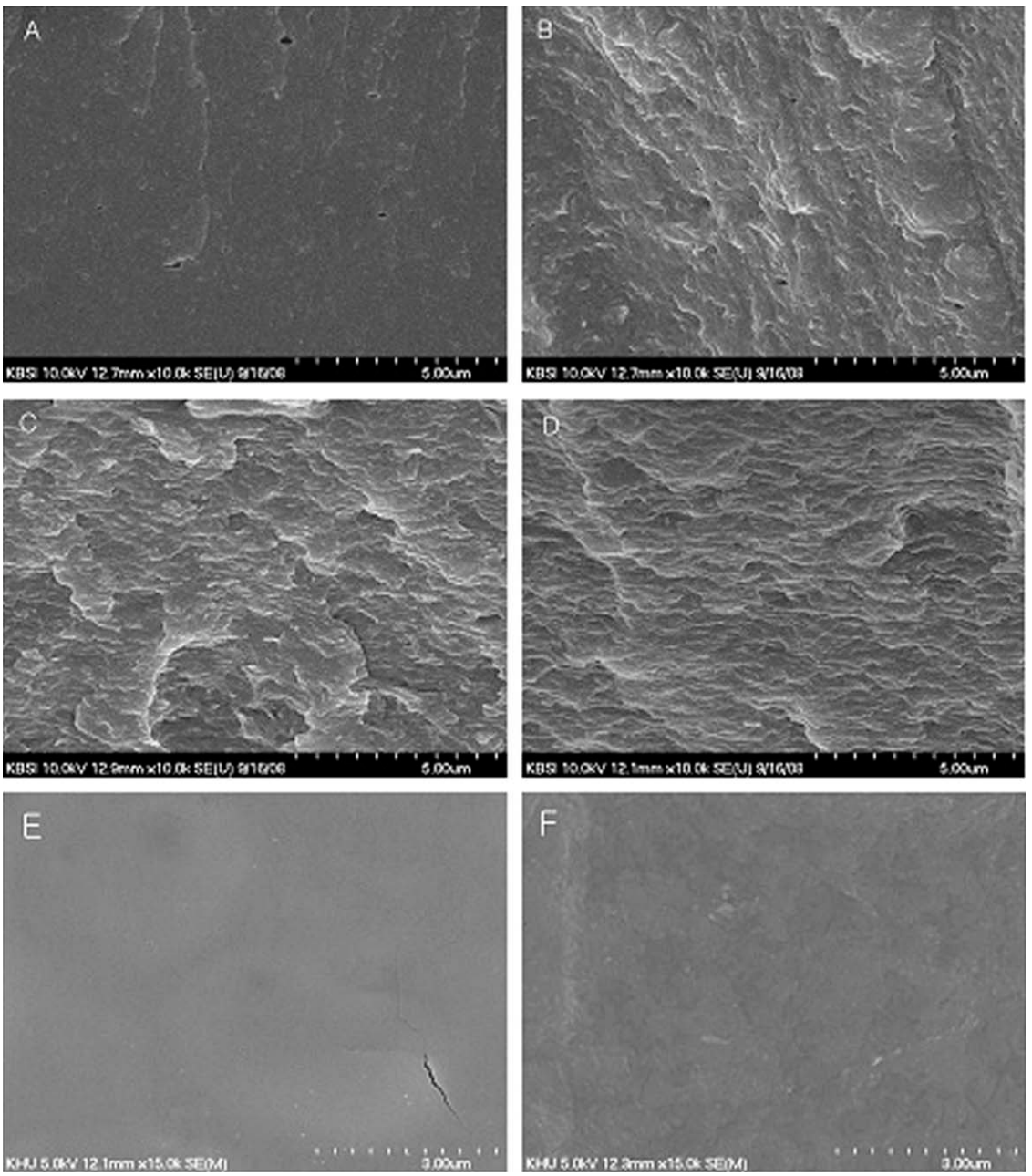

Figure 5 SEM images of SPI/MMT composite films (A-D: cross-section; E and F: surface). (A) SPI film. (B) SPI-3% MMT composite film. (C) SPI-9% MMT composite film. (D) SPI-15% MMT composite film. (D) SPI film. (E) SPI-15% MMT composite film.

absence of the basal peak of $2\theta \approx 8^\circ$, implying that the clay was destroyed and an intercalated nanocomposite had been formed (Fig. 4). The intensity of MMT peak at $2\theta \approx 20^\circ$ decreased after incorporating with SPI solution, but a sharper peak pattern was observed at 15% MMT in SPI film. Decreasing peak intensity and broadening peak mostly indicate an intercalated or exfoliated structure, while increasing peak intensity and sharp peak indicate the formation of crystallinity, which explains why the 15% MMT-SPI film had the highest tensile strength and OP. Peak shifting to a lower angle also was observed with a spacing of $2\theta \approx 8^\circ$ to $2\theta \approx 3^\circ$ in SPI-MMT composite films with MMT content ranging from 3% to 15%. Cyras et al.[17] observed the peak shift to lower angles regardless the clay content in starch-MMT composite films, and asserted that either the glycerol or the polymer chains, or both, entered into the silicate layers forming an intercalated starch/MMT nanocomposite. Park et al.[26] explained that changes of crystallinity could be due to the strong polar interactions between the hydroxyl groups present both in the biopolymer chain, glycerol, and in the silicate layers of starch/MMT composites.

Presently, the spacing distance values increased from 2.31 nm to 2.58 nm as the MMT content increased from 3% to 12%, thereafter decreasing to 2.41 nm at 15% MMT. This evidently indicates the adoption of a more crystalline structure in SPI films on the addition of 15% MMT, and entirely explains the high OP of the latter films.

SEM

SEM images of SPI/MMT composite films [Fig. 5(A–F)] demonstrated a smoother morphology in fractured cross-section at 15% MMT as compared to 3% or 9% MMT. Totally, different morphology in cross-section and surface was observed after MMT was added into SPI films. The granular shape of SPI-MMT composite films was consistent with some crystalline behavior at high levels of incorporated MMT. The SEM views of fractured cross sections and surfaces of film were indicative of clustering. Cavities observed in MMT-free SPI films [Fig. 5(A)] were likely caused by dissolved air, while no clustering and cavities were found in cross sections of SPI films incorporating 15% MMT [Fig. 5(D)]. This indicates that intercalated nano materials filled the SPI polymer, which is consistent with the significant ($P < 0.05$) WVP and OP of SPI/MMT composite films.

SUMMARY AND CONCLUSIONS

Soy protein is a promising biodegradable polymer for active food packaging. However, because of its mechanical and barrier inferiority to petroleum-based films, its application is presently hampered. In previous works, many researches have concentrated on the improvement of functionality of SPI film but no decision of optimal MMT concentration into SPI film was made. In present study, a series of nanocomposite films consisting of SPI and MMT clay were prepared by effectively dispersal via sonication and homogenization. We obtained biodegradable SPI films that were completely constructed from renewable resources. MMT nanoparticles significantly increased TS and decreased *E*, WVP, and, partially, OP, whereas no significance of TSM was evident. An optimal addition content range of 3%–12% (w/w of SPI), MMT was required to improve the functional properties of SPI-MMT composite films. Mechanical properties among the other functionalities was much improved compared with previous studies of gluten/MMT-[10], SPI/clay mineral-[12], and WPI/clay-composite films.[11] This effect can be attributed to a different structuring of protein network in the presence of layered silicates; the new structuring of protein-MMT composite may be affected by intercalation of MMT particles and interaction between nano silicates and protein molecules in solution. The Na-MMT layers were intercalated as evidenced by XRD examination and its clustered morphology was observed by SEM. Intercalation can be assumed by changes of peak intensity and shifting in X-ray diffraction patterns of pure Na-MMT, SPI film, and SPI-MMT composite films.

References

1. McGalshan, S. A.; Halley, P. J. Polym Int 2003, 52, 1767.
2. Rhim, J. W. Korean J Food Sci Technol 1998, 30, 372.
3. Kim, K. M.; Marx, D. B.; Weller, C. L.; Hanna, M. A. J Am Oil Chem Soc 2003, 80, 71.
4. Gennadios, A.; Rhim, J. W.; Handa, A.; Weller, C. L.; Hanna, M. A. J Food Sci 1998, 63, 225.
5. Rhim, J. W.; Gennadios, A.; Fu, D.; Weller, C. L.; Hanna, M. A. LWT—Food Sci Technol 1999, 32, 129.
6. Kim, K. M.; Hanna, C.L.W.; Gennadios, A. J Food Sci 2002, 67, 708.
7. Motoki, M.; Nio, N.; Takinami, K. Agric Biol Chem 1987, 51, 237.
8. Stuchell, Y. M.; Krochta, J. M. J Food Sci 1994, 59, 1332.
9. Yildirim, M.; Hettiarachchy, N. S. J Food Sci 1997, 62, 270.
10. Tunc, S.; Angellier, H.; Cahyana, Y.; Chalier, P.; Gontard, N.; Gastaldi, E. J Membr Sci 2007, 289, 159.
11. Sothornvit, R.; Rhim, J. W.; Hong, S. J Food Eng 2009, 91, 468.
12. Rhim, J. W.; Lee, J. H.; Kwak, H. S. Food Sci Biotechnol 2005, 14, 112.
13. ASTM. Standard test methods for tensile properties of thin plastic sheeting. In: Annual Book of ASTM Standards. American Society for Testing and Materials: West Conshohochen, PA, 1995; Vol. 8.01.
14. ASTM. Standard test methods for water vapor transmission of materials. In: Annual Book of ASTM Standards. American Society for Testing and Materials: Philadelphia, PA, 1995; Vol. 4.06.
15. Dean, K.; Yu, L.; Wu, D.Y. Compos Sci Technol 2007, 67, 413.
16. Jiang, L.; Zhang, J.; Wolcott, M. P. Polymer 2007, 48, 7632.
17. Cyras, V. P.; Manfredi, L. B.; Ton-That, M. T.; Vázquez, A. Carbohydr Polym 2008, 73, 55.
18. Xu, Y.; Ren, X.; Hanna, M. A. J Appl Polym Sci 2006, 99, 1684.
19. Krook, M.; Morgan, G.; Hedenqvist, M. S. Polym Eng Sci 2005, 45, 135.
20. Yu, T.; Lin, J.; Xu, J.; Chen, T.; Lin, S.; Tian, X. Compos Sci Technol 2007, 67, 3219.
21. Krishnamoorti, R.; Vaia, R. A.; Giannelis, E. P. Chem Mater 1996, 8, 1728.
22. Olabarrieta, I.; Gällstedt, M.; Ispizua, I.; Sarasua, J. R.; Hedenqvist, M. S. J Agric Food Chem 2006, 54, 1283.
23. Shah, R. K.; Krishnaswamy, R. K.; Takahashi, S.; Paul, D. R. Polymer 2006, 47, 6187.
24. Michaels, A. S.; Bixler, H. J. J Polym Sci 1961, 50, 393.
25. Döppers, L. M.; Breen, C.; Sammon, C. Vib Spectrosc 2004, 35, 27.
26. Park, H. M.; Li, X.; Jin, C. Z.; Park, C. Y.; Cho, W. J.; Ha, C. S. Macromol Mater Eng 2002, 287, 553.